Calculation of Doublet Capture Rate for Muon Capture in Deuterium within Chiral Effective Field Theory

J. Adam, Jr., M. Tater, and E. Truhlík

Institute of Nuclear Physics ASCR, CZ–250 68 Řež, Czech Republic

E. Epelbaum

Institut fuer Theoretische Physik II,
Fakultaet fuer Physik und Astronomie,
Ruhr-Universitaet Bochum, 44780 Bochum, Germany

R. Machleidt

Department of Physics, University of Idaho, Moscow, ID 83844-0903, USA

P. Ricci

Istituto Nazionale di Fisica Nucleare, Sezione di Firenze,
I-50019 Sesto Fiorentino (Firenze), Italy

Abstract

The doublet capture rate $\Lambda_{1/2}$ of the negative muon capture in deuterium is calculated employing the nuclear wave functions generated from accurate nucleon-nucleon (NN) potentials constructed at next-to-next-to-next-to-leading order of heavy-baryon chiral perturbation theory and the weak meson exchange current operator derived within the same formalism. All but one of the low-energy constants that enter the calculation were fixed from pion-nucleon and nucleon-nucleon scattering data. The low-energy constant $\hat{d}^R$ (c_D), which cannot be determined from the purely two-nucleon data, was extracted recently from the triton β-decay and the binding energies of the three-nucleon systems. The calculated values of $\Lambda_{1/2}$ show a rather large spread for the used values of the $\hat{d}^R$. Precise measurement of $\Lambda_{1/2}$ in the future will not only help to constrain the value of $\hat{d}^R$, but also provide a highly nontrivial test of the nuclear chiral EFT framework. Besides, the precise knowledge of the constant $\hat{d}^R$ will allow for consistent calculations of other two-nucleon weak processes, such as proton-proton fusion and solar neutrino scattering on deuterons, which are important for astrophysics.

PACS numbers: 12.39.Fe; 21.45.Bc; 23.40.-s

Keywords: negative muon capture; deuteron; effective field theory; meson exchange currents

I. INTRODUCTION

The weak nuclear interaction plays crucial role in the formation of stars in our Universe: it starts the pp chain of the solar burning. In this chain, the following reactions occur, triggered by the weak nuclear interaction [1],

$$p + p \rightarrow d + e^+ + \nu_e\,, \tag{1.1}$$
$$p + p + e^- \rightarrow d + \nu_e\,, \tag{1.2}$$
$$p + {}^3He \rightarrow {}^4He + e^+ + \nu_e\,, \tag{1.3}$$
$${}^7Be + e^- \rightarrow {}^7Li + \nu_e\,, \tag{1.4}$$
$${}^8B \rightarrow {}^8Be^* + e^+ + \nu_e\,. \tag{1.5}$$

The neutrinos produced in these reactions are messengers from the very core of the Sun, where the hydrogen burning occurs. Therefore, their study can provide a valuable information on star formation. The neutrinos, released in reaction (1.5) have a continuous spectrum with the maximum energy 15 MeV and have recently been registered in the SNO detector [2–4] via the reactions

$$\nu_x + d \rightarrow \nu_x' + n + p\,, \tag{1.6}$$
$$\nu_e + d \rightarrow e^- + p + p\,, \tag{1.7}$$

also induced by the weak nuclear interaction. As a result, the registered neutrino flux for the neutral current reaction (1.6) confirmed the validity of the Standard Solar Model. Simultaneously, the neutral current to charged current ratio [3] established unambiguously the presence of an active neutrino flavor other than ν_e in the observed solar neutrino flux, thus confirming definitely the phenomenon of the neutrino oscillations and that the neutrinos possess a finite mass.

It is clear that the precise description of reactions (1.1)-(1.7) is of fundamental value. However, the reactions (1.1)-(1.7) cannot be studied experimentally at present with desired accuracy in terrestrial conditions. In order to perceive them, one should address other weak processes in few-nucleon systems that are feasible in laboratories, such as

$${}^3H \rightarrow {}^3He + e^- + \bar{\nu}_e\,, \tag{1.8}$$
$$\mu^- + {}^3He \rightarrow {}^3H + \nu_\mu\,, \tag{1.9}$$
$$\mu^- + d \rightarrow n + n + \nu_\mu\,. \tag{1.10}$$

Then, relying on the cosmological principle, one can apply the acquired knowledge on the weak nuclear interaction also to other weak processes, occurring in the extraterrestrial conditions. The reactions (1.8) and (1.9) have already been studied experimentally in great detail. The half-life of the triton is known with an accuracy ~ 0.3 %, $(fT_{1/2})_t = (1129.6 \pm 3)$ s [5], and the capture rate of muon on ^{3}He (1.9), $\Lambda_0 = 1496 \pm 4$ sec^{-1} [6, 7] is also known with the same accuracy. The situation with the reaction (1.10) is less favorable so far. Indeed, the last measurements of the doublet capture rate provided $\Lambda_{1/2} = 470 \pm 29$ sec^{-1} [8] and $\Lambda_{1/2} = 409 \pm 40$ sec^{-1} [9]. This unfavorable situation is expected to change soon in view of a precision experiment planned by the MuSun Collaboration [10], whose goal is to measure

$\Lambda_{1/2}$ with an accuracy of ~ 1.5 %. Keeping in mind that the two-nucleon system is much simpler than the three-nucleon one such a precise knowledge of $\Lambda_{1/2}$ will help to clarify best the situation in the theory of reactions triggered by weak nuclear interaction in few-nucleon systems.

The main theoretical problem concerning the above quoted nuclear reactions is caused by the non-perturbative nature of quantum chromodynamics (QCD) at low energies. The way of handling this obstacle has already been outlined 50 years ago by realizing that the description of the electro-weak interaction with a nuclear system, containing nucleons and pions, should be based on the spontaneously broken global chiral symmetry $SU(2)_L \times SU(2)_R$, reflected in the QCD Lagrangian [11, 12], see also [13, 14]. Later on, a concept of hidden local symmetry allowed one to extend the nuclear system to contain also heavy mesons [15, 16]. The nonlinear chiral Lagrangians [17–20] served then as a starting point for constructing the one-boson exchange currents in the tree approximation. The reactions (1.6)-(1.10) were studied with such currents in Refs. [21–28]. Calculations [20–22, 25, 28] were performed with the nuclear wave functions derived from one-boson exchange potentials [29, 30], thus providing rather consistent results. We refer to this concept as Tree Approximation Approach (TAA). In the more general Standard Nuclear Physics Approach (SNPA) [31], one employs realistic nucleon-nucleon (NN) potentials which usually have no relation to applied meson-exchange currents thus lacking the consistency. Generally, these concepts describe well the nuclear phenomena triggered by the electro-weak interaction up to energies ~ 1 GeV [32–40].

The crucial step allowing one to go beyond the tree approximation was made by Weinberg [41]. In this work, Weinberg formulated the principles of chiral perturbation theory (χPT) which is an effective field theory (EFT) of QCD at low energies. The effective chiral Lagrangian is constructed by including all possible interactions between pions and nucleons consistent with the symmetries of QCD and, especially, the spontaneously broken approximate chiral symmetry. Weinberg also established counting rules [42, 43] allowing one to classify the contribution of various terms of perturbative expansion in positive powers of q/Λ_χ, where q is a momentum or energy scale of the order of the pion mass characterizing a given hadronic system which is small in comparison with the chiral symmetry breaking scale $\Lambda_\chi \sim 1$ GeV.

In order to calculate reliably the capture rates and cross sections of reactions one needs to know accurately the current operators and the nuclear wave functions (potentials). The weak axial currents were studied within the EFT in Refs. [44, 45]. At leading- (LO) and the next-to-leading (NLO) orders, the weak nuclear current consists of the well-known single nucleon terms [46, 47]. The space component of the weak axial meson-exchange current (MEC), which contributes to observables in all weak reactions mentioned above and is, therefore, of the main interest here, appears first at N^{3}LO. It involves one unknown constant $\hat{d}^R$,

$$\hat{d}^R \,=\, \hat{d}_1 \,+\, 2\hat{d}_2 + \,\frac{1}{3}\,(\hat{c}_3 \,+\, 2\hat{c}_4) \,+\, \frac{1}{6}\,, \tag{1.11}$$

where the dimensionless constants $\hat{c}_i$ and $\hat{d}_j$ are given by

$$\hat{c}_i \,=\, M_N\, c_i\,, \quad i = 1, \ldots, 4\,, \quad \hat{d}_j \,=\, -\frac{M_N f_\pi^2}{g_A}\, d_j\,, \quad j = 1, 2\,, \tag{1.12}$$

with c_i and d_j being the low-energy constants (LECs) entering the chiral Lagrangian of the πNN system at the NLO [44, 45]. Further, M_N=0.939 GeV is the nucleon mass, g_A is the nucleon axial vector coupling constant and f_π denotes the pion decay constant. The linear combination $\hat{d}_1 + 2\hat{d}_2$ is often replaced by an effective LEC c_D [48],

$$\hat{d}_1 + 2\hat{d}_2 = -\frac{M_N}{\Lambda_\chi g_A} c_D \,, \tag{1.13}$$

where $\Lambda_\chi = 0.7$ GeV.

Let us note that the weak axial currents [44, 45] were derived without referring to any equation describing nuclear states. The resolution of the problem of double counting in conjunction with the Schroedinger equation [49] provided a weak axial pion potential current, the presence of which ensures that the weak axial MECs satisfy the nuclear PCAC constraint,

$$q_\mu j^a_{5\mu}(2,\vec{q}) = +([\, V_\pi \,,\, \rho^a_5(1,\vec{q})\,] + (1 \leftrightarrow 2)) + i f_\pi m^2_\pi \Delta^\pi_F(q^2)\, M^a_\pi(2,\vec{q}) \,. \tag{1.14}$$

Here V_π is the one-pion exchange potential, $\rho^a_5(1)$ is the one-nucleon axial charge density, m_π is the pion mass, $\Delta^\pi_F(q^2)$ is the pion propagator and $M^a_\pi(2)$ is the two-nucleon pion absorption/production amplitude. The weak axial potential current is not a part of the weak axial currents of Refs. [44, 45].

Eq. (1.14) is a direct analogue of the nuclear conserved vector current constraint valid for the weak vector MECs,

$$q_\mu j^a_\mu(2,\vec{q}) = ([\, V_\pi \,,\, \rho^a(1,\vec{q})\,] + (1 \leftrightarrow 2)) \,. \tag{1.15}$$

The consistency of calculations requires that both potentials and currents are derived from the same Lagrangian. Presently, only few calculations of weak reactions performed within the EFT approach fulfill this requirement. Instead, one often adopts the so-called "hybrid" approach in which the current operator is constructed from the EFT as outlined above but the wave functions are generated either from the one-boson-exchange potentials of the TAA [30, 50] or from purely phenomenological potentials [51]. Notice that all these potentials describe low-energy NN scattering data with χ^2/data ≈ 1. Besides, when calculating observables for the weak processes in the three- and more nucleon systems (see below), also the three-nucleon forces [52, 53] were addressed. So far, almost all calculations aiming to study the weak interaction in few-nucleon systems made use of the precisely known half-life of the triton to extract $\hat{d}^R$. In this way, this constant was determined in Ref. [54] from the reduced Gamow-Teller (GT) matrix element for the reaction (1.8), and then the spectroscopic factors $S_{pp}(0) = 3.94 \times (1 \pm 0.004) \times 10^{-25}$ MeV b and $S_{hep}(0) = (8.6 \pm 1.3) \times 10^{-30}$ keV b were calculated for reactions (1.1) and (1.3), respectively. Using the same values of $\hat{d}^R$, the doublet capture rate $\Lambda_{1/2} = 386$ sec^{-1} for the reaction (1.10) was obtained in Ref. [55] and the cross sections of the reactions (1.6) and (1.7) were calculated in Ref. [56]. Let us note that the authors [54] employed purely phenomenological 2N AV18 [51] and 3N Urbana-IX [53] potentials. Similarly, in Ref. [57], the capture rate $\Lambda_0 = 1499 \pm 16$ sec^{-1} for the reaction (1.9) was obtained based on the same potentials. In Ref. [58], Marcucci and Piarulli employed AV18 NN potential to generate the nuclear wave functions for the

process ^{2}H(μ^-, ν_μ)nn and AV18 + Urbana IX 3N potentials for the reaction ^{3}He$(\mu^-, \nu_\mu)^3$H. The weak current was taken from the χPT approach with the weak axial potential current of Ref. [49] added. The calculations resulted in $\Lambda_{1/2} = 393.1 \pm 0.8$ s^{-1} and $\Lambda_0 = 1488 \pm 9$ s^{-1}.

The problem with the above mentioned hybrid calculations is that they do not allow for a simultaneous determination of the LECs c_D and c_E which govern the short-range part of the 3NF at N^{2}LO. More precisely, the constant c_D enters not only the weak axial MEC, but also the contact and one-pion exchange part of the three-nucleon force whereas the constant c_E controls the strength of the three-nucleon contact term [48, 59]. These LECs can be determined by purely hadronic few-nucleon observables such as e.g. the triton binding energy and the nucleon-deuteron doublet scattering length [48] or the spectra of light nuclei [60]. Strong correlations between various few-nucleon observables such as e.g. the Philips and Tjon lines, however, often prevent from a precise determination of these LECs. On the other hand, a recent determination of these LECs from the triton binding energy and the half life [61] seems to be more robust in this sense.

We also mention a recent work [28], where the values of $\Lambda_{1/2}$ for the reaction (1.10) were calculated within the TAA. The nuclear wave functions were derived from the Nijmegen I and Nijmegen 93 potentials [30] and the exchange current models were constructed within the approach of hidden local symmetry [20]. Taking these capture rates as input, then the values of $\hat{d}^R$ were extracted in the hybrid approach, in which the nuclear wave functions were kept the same as in TAA and the weak axial MECs were taken from the χPT approach [44].

The reactions of muon capture in deuterium and in ^{3}He have recently been studied by the Pisa group [62] in the SNPA- and hybrid approaches and within the χPT as well. The resulting values of the capture rates are, $\Lambda_{1/2} = (389.7$ - $394.3)$ s^{-1} and $\Lambda_0 = (1471$ - $1497)$ s^{-1}. Subsequent calculations by this group [63] within the χPT provided $\Lambda_{1/2} = 400 \pm 3$ s^{-1} and $\Lambda_0 = 1494 \pm 21$ s^{-1}. We will make a more detailed comparison with these results in the next section.

Recently, accurate NN potentials at N^{3}LO by Epelbaum, Glöckle and Meißner (EGM) [64] and Entem and Machleidt (EM) [65] have become available. In both cases, the parameters entering the calculations are standardly extracted from the fit to the NN scattering data and the deuteron properties, or taken from the analysis of the πN scattering.

The EGM and EM potentials differ from each other in several aspects. First, EGM adopted the so-called spectral function regularization [66] of the two-pion exchange contributions, while the analysis by EM is based upon dimensionally regularized expressions. Further differences can be attributed to the implementation of the momentum-space cutoff in the Schroedinger equation, the treatment of relativistic and isospin-breaking effects as well as the fitting procedure: the LECs, accompanying the contact interactions, were determined by EM by fitting directly to the scattering data, whereas EGM extracted them by the fit to the Nijmegen PWA. For more details we refer the reader to the original publications [64, 65] and to the review articles [67, 68].

In its turn, the simultaneous extraction of the constants c_D and c_E has recently been carried out in Ref. [61], where these constants have been constrained by calculations of the binding

energies of the three-nucleon systems and of the reduced GT matrix element of the triton β decay. The nuclear wave functions were generated in accurate *ab initio* calculations using both the two-nucleon N^{3}LO EM [65] and three-nucleon N^{2}LO force [48, 59], whereas the reduced GT matrix element of the process (1.8) has been calculated with the two-nucleon weak axial MECs, derived from the same χPT Lagrangian [57] as the nuclear forces. Besides, the calculations with two versions of the EGM potential have also been performed (without, however, taking into account the three-nucleon force). The resulting values of c_D cover two rather distinct intervals (see Table IV).

In this work, we use the results of Ref. [61] for c_D to calculate $\Lambda_{1/2}$. We apply the same potentials for generating the deuteron and neutron-neutron (nn) wave functions and the weak axial MEC operator, equivalent to that used in Ref.[61], thus obtaining a rather consistent prediction for the values of $\Lambda_{1/2}$, falling correspondingly into two rather different sets. Based on these results we conclude that a precise measurement of $\Lambda_{1/2}$ (i) will provide a highly nontrivial consistency check for the chiral EFT approach and (ii) using the extracted values of c_D ($\hat{d}^R$), will allow to calculate consistently other two-nucleon weak processes, such as proton-proton fusion and solar neutrino scattering on deuterons, which are important for astrophysics. Besides it turns out [69] that $\hat{d}^R$ enters also the capture rate for the reaction $\pi^- + d \to \gamma + 2\,n$, which is the best source of information on the nn scattering length a_{nn}, see also a related work by Lensky et al. [70].

In addition, we employ the weak axial pion potential current [49] and study its influence on the values of $\Lambda_{1/2}$ and $\hat{d}^R$ as well. As we shall see, its contribution to $\Lambda_{1/2}$ is at the level of the weak axial exchange charge density. Therefore, it should be necessarily taken into account in the analysis of $\Lambda_{1/2}$. Since this current was omitted in Ref. [61], its influence on extraction of c_D from the GT matrix element for the reaction (1.8) is not clear.

Our manuscript is organized as follows. In Section II, we discuss briefly the methods and inputs necessary for the calculations, in Section III, we present the results and discussion and we conclude in Section IV. In Appendix A, we give a short description of our treatment of the nn wave functions within the K-matrix method and in Appendix B, the form factors, arising after the Fourier transformation of the weak MECs in presence of the regulator of the type (2.2), are delivered.

II. METHODS AND INPUTS

Here we present the necessary ingredients of the calculations of $\Lambda_{1/2}$. They concern the used potentials, the method of generation of the nn wave functions, and the EFT currents.

A. Nuclear potentials and wave functions

In our calculations of nuclear matrix elements we start, in accordance with Ref. [61], by adopting the N^{3}LO EM and two species of the EGM(ORC) potential with the parameters $O = 2$, $R = 0$ and $C = 4, 5$. The meaning of these parameters is as follows: (i) $O = 2$ means

TABLE I: The scattering length a_{nn} (in fm), and the effective range r_{nn} (in fm), calculated for the $^1S_0$ channel from the used potentials.

$^1S_0$ *wave*	a_{nn}	r_{nn}	a_{nn}^{exp}	r_{nn}^{exp}
EM	-18.89	2.84		
EGM(204)	-18.90	2.78	-18.9 $\pm$ 0.4 [a])	2.75 $\pm$ 0.11 [b])
EGM(205)	-18.91	2.88		

[a]) Ref. [71] [b]) Ref. [72]

TABLE II: Deuteron properties derived from the EM and EGM(204) and EGM(205) chiral potentials. Here E_d is the deuteron binding energy in MeV, P_d is the D-state probability in %, $< \mu >_z$ is the deuteron magnetic moment in the nuclear Bohr magnetons, Q_d is the deuteron quadrupole moment in fm^2, $\sqrt{<}r^2>$ is the deuteron root-mean-square radius in fm, A_S is the asymptotic normalization factor of the S-state in fm$^{-1/2}$ and η_d is the asymptotic D/S ratio. The magnetic and quadrupole moments are calculated in the impulse approximation.
Experimental values of these quantities are: E_d=-2.224575(9) MeV [73], $< \mu >_z$=0.8574382284(94) [74], Q_d=0.2859(3) fm^2 [75], $\sqrt{<}r^2>$=1.9753(11) fm [76], A_S=0.8846(9) fm$^{-1/2}$ [75], and η_d=0.0256(4) [77].

Deuteron	E_d	P_d	$< \mu >_z$	Q_d	$\sqrt{<}r^2>$	A_S	η_d
EM	-2.224575	4.52	0.8540	0.2753	1.9750	0.8843	0.0256
EGM(204)	-2.218923	2.84	0.8635	0.2659	1.9856	0.8829	0.0254
EGM(205)	-2.223491	3.63	0.8590	0.2692	1.9754	0.8833	0.0255

that the potential is constructed at order N^{3}LO. (ii) The value $R = 0$ provides the potential for the usual non-relativistic Lippmann-Schwinger equation. (iii) The value of $C = 4(5)$ defines the choice of the cutoff used in the Lippmann-Schwinger equation to be 450 MeV (600 MeV) and of the cutoff in the spectral function representation of the two-pion potential to be 700 MeV (700 MeV). The *nn* wave functions in the continuum were generated by the K(R)-matrix method [50, 78]. The basic equations are detailed in Appendix A.

For a reliable evaluation of $\Lambda_{1/2}$, the potential should describe precisely the scattering length a_{nn} and the effective range r_{nn} in the $^1S_0$ channel of the *nn* system. In Table I, we present these quantities for the used potentials, together with the experimental values. We also present in Table II the properties of the used deuteron wave functions. Last but not least, we emphasize that in the calculations of $\Lambda_{1/2}$, the nn $^{2S+1}L_{j_f}$ partial waves with L=0,1,2,3 and j_f=0,1,2 are taken into account.

B. Weak nuclear MECs

The weak axial MECs constructed within the HBχPT [44] and used in our calculations are discussed in detail in Section 2.2 of Ref. [28]. We present in Table III only the LECs necessary for the calculations of $\Lambda_{1/2}$.

The LECs c_i can be obtained from πN scattering, see Ref. [79] and references therein. There have been also attempts to determine these LECs from two-nucleon scattering data [80]. Notice that NN N^{3}LO potentials of Refs. [64, 65] adopt different values for the LEC c_4. In particular, in [65] the value of this LEC was tuned to improve the description of the NN data. We further emphasize that the LECs $c_{2,3,4}$ receive important contributions from the $\Delta(1232)$ isobar in the process of fixing them via saturation by higher resonances, see Refs. [81, 82].

TABLE III: Values of the LECs c$_i$ (in GeV^{-1}) adopted in the N^{3}LO potentials [64, 65].

Potential	c$_1$	c$_2$	c$_3$	c$_4$	c$_6$
EM	-0.81	2.80	-3.20	5.40	3.70
EGM	-0.81	3.28	-3.40	3.40	3.70

In the EM model, values of c_4 between 3.40 and 5.40 GeV^{-1} are admissible [65]. As discussed above, the unknown LECs $\hat{d}_1$ and $\hat{d}_2$, entering the weak axial MECs, are connected with the LEC c_D by Eq. (1.13). In addition, we also include the weak axial pion potential current of Eq. (A.17) [28], required by the PCAC constraint (1.14).

The parameter $\hat{d}^R$ (c_D) manifests itself in the two-nucleon contact vertex of the weak axial current, representing a short range component of the MEC (see Fig. 1). Besides, it is also present in a short-range part of the three-nucleon force. Fixing this LEC from some few-nucleon processes feasible in laboratory allows one to make model independent predictions for other weak processes (at the given order) triggered by this component of the weak axial current. We further emphasize that the time component of the weak axial MEC depends only on the known LECs c_2 and c_3 at the same chiral order.

Besides these weak axial MECs, we include also the weak vector MECs of the pion range: the π-pair term, the pion-in-flight term and the Δ excitation current of the π range, given in Eqs. (A.9), (A.10) and (A.11), respectively [28]. Their derivation is and properties are discussed in detail in Sections 2.1 and 2.2 of Ref. [28]. Let us note that the model independent longitudinal π-pair and pion-in-flight terms, fixed by the low energy theorem, satisfy the nuclear conserved vector current constraint (1.15), whereas the current (A.11) is transverse and, therefore, model dependent.

On the other hand, the leading order electromagnetic MECs were obtained within the HBχPT approach for the πN system in Ref. [83], where they were referred to as "generalized tree graphs". From these currents, the weak vector currents are derived by rotating in the isospin space. They are given in Eqs. (35) and (42) [83]. It is straightforwardly seen that our π-pair and pion-in-flight currents coincide with the currents of Eq. (35) and the Δ

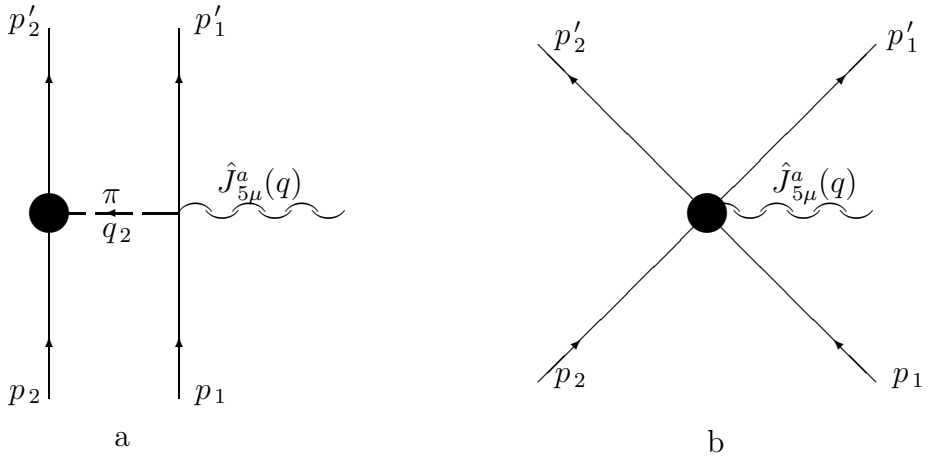

FIG. 1: The general structure of the two–nucleon weak axial operators; a– the long-range operator, b– the short-range operator.

excitation current with the part of the current of Eq. (42) proportional to the LEC c_9, saturated by the Δ isobar (see Eq. (43) [83]) *. Moreover, the same currents were obtained in the Appendix C of the same Ref. [83] from an effective chiral Lagrangian of the $\pi N\Delta\rho\omega$ system formulated in the heavy-fermion formalism. The most modern derivation of the electromagnetic MECs [84, 85], based on the chiral effective theory of the πN system and the method of unitary transformation, again provides the leading order currents of the above discussed form (see Eq. (4.28) [85]). These currents contain some LECs, from which so far only $\bar{d}_{18}$ has been reliably fixed. The natural identification of the leading order terms, proportional to $\bar{d}_{18}$, with the standard π-pair and pion-in-flight currents leads to

$$\bar{d}_{18} = -1/4m_\pi^2 = -12.8\, GeV^{-2}. \tag{2.1}$$

On the other hand, the value of $\bar{d}_{18}$ was fixed in Ref. [86] by the Goldberger-Treiman discrepancy with the result $\bar{d}_{18}$=-10.14$\pm$0.45 GeV^{-2}, which is in a good agreement with the value (2.1), predicted by the low energy theorem. The other LECs, related to the transverse part of the discussed current are not yet well known. Natural way to extract them seems to be the study of pion photo- and electro-production, or capture reactions. One can also proceed by fixing them via saturation by the resonances, as it was done in Ref. [83].

It should be clear from our discussion that the leading order vector MECs of the pion range are determined by chiral invariance uniquely. Therefore, working with these MECs in this approximation, we can use safely our currents in the calculations done here.

In accord with Ref. [61], we multiply the MECs by the regulator

$$F_\Lambda^n(q^2) \,=\, e^{-(q/\Lambda)^{2n}}\,, \quad n=2\,, \quad \Lambda = 0.5\,\mathrm{GeV}\,, \tag{2.2}$$

* Another part of the current of Eq. (42) is proportional to the LEC c_7^R, which is obtained by saturation by the ω meson. As it is seen from Table 2 [83], the contribution from this current to the reduced matrix element for the radiative neutron capture on proton is minor and we do not consider it.

TABLE IV: Calculated values of $\Lambda_{1/2}$, $\bar{\Lambda}_{1/2}$ and of the MECs effect δMECs=$\Lambda_{1/2}$ -$\Lambda_{1/2}$ (IA) (in s^{-1}) for the chiral potentials EM [65] and EGM [64]. The capture rate $\bar{\Lambda}_{1/2}$ differs from $\Lambda_{1/2}$ by taking into account the weak axial pion potential current. The intervals of allowed values of c_D are taken from Refs. [61, 87], the corresponding values of $\hat{d}^R$ are derived using Eq. (1.11) and c_i from Table III.
EM^a (EM^b)- the EM potential with c_4=3.4 (5.4) GeV^{-1}.

	EM^a		EM^b		EGM(204)		EGM(205)	
c_D	−0.05	0.2	−0.3	−0.1	0.05	0.33	3.30	4.20
$\hat{d}^R$	1.18	1.44	2.23	2.44	1.28	1.57	4.66	5.60
$\Lambda_{1/2}$	383.8	387.2	389.4	392.4	386.4	389.1	410.1	419.1
$\bar{\Lambda}_{1/2}$	381.6	385.1	387.2	390.1	385.2	387.9	408.3	417.1
δMECs	4.2	7.6	9.8	12.4	2.1	4.7	29.9	38.5

keeping the currents local in configuration space. The form factors arising after the Fourier transform of the currents are given in Appendix B.

III. RESULTS AND DISCUSSION

The calculation of $\Lambda_{1/2}$ is discussed in detail in Section 3 of Ref. [28]. Its value is obtained from the equation

$$\Lambda_{1/2} \,=\, \Lambda_{stat} \,+\, \delta\,\Lambda/3\,, \tag{3.1}$$

where Λ_{stat} and $\delta\,\Lambda$ are given in Eqs. (3.2) and (3.7) [28], respectively. The results for $\Lambda_{1/2}$ are displayed in Table IV. As it is seen from Table IV, the values of $\Lambda_{1/2}$ are located in two rather distinct intervals. For the NN potentials EM and EGM(204), they are in the interval 383.8 $s^{-1} \leq \Lambda_{1/2} \leq$ 392.4 s^{-1}, thus featuring a spread of about 2%. The spread of the values of $\Lambda_{1/2}$ obtained in the EGM(205) model is about the same, but these values are larger by $\approx$ 6 % and the MECs effect is also much larger. If one would like to get within the model EGM(205) the value $\Lambda_{1/2}$ =389.1 s^{-1}, one should take $\hat{d}^R$ =2.35 corresponding to c_D=1.08 which is far out of the interval $3.30 \leq c_D \leq 4.20$ allowed by the reduced GT matrix element of the triton β decay.

One can see from Table IV that the presence of the weak axial pion potential current suppresses $\Lambda_{1/2}$ up to 0.5 %. E.g., in the case of the model EM^b and for the value $\hat{d}^R$ (c_D) =2.23 (-0.3), one gets $\Lambda_{1/2}$ =389.4 s^{-1}, whereas $\bar{\Lambda}_{1/2}$ =387.2 s^{-1}. This difference in the capture rate can be reflected in the change of $\hat{d}^R$ (c_D) = 2.07 (-0.45), which means the change of $\sim$ 7.5 % (44 %) in $\hat{d}^R$ (c_D).

Let us now discuss for the same model EM^b the variation of extracted $\hat{d}^R$ (c_D), if the supposed experimental value of $\Lambda_{1/2}$ =390 $\pm$6 s^{-1} is measured with an accuracy of 1.5 %. The extracted value of $\hat{d}^R$ =2.27$\pm$0.44, to which corresponds c_D=-0.26$\pm$0.42. It is seen that the value of $\hat{d}^R$ (c_D) would be known with an accuracy of 20 % (140 %). With the weak axial

pion potential current included, the interval of $\hat{d}^R$ (c_D) would be shifted to the negative values by ~ 7.5 % (44 %) as a whole.

In Table V, we give individual contributions of various components of the currents, the multipoles of which can be found in Appendix C of Ref. [28]. For the EGM version, the contribution of the weak axial pion potential current $\vec{\jmath}_A$(p.p.c.) is about the same as that of the time component of the weak axial MECs, and for the EM potentials it is twice as large. Notice that in the calculations of [28] based on the Nijmegen I potential [30], the suppression of $\Lambda_{1/2}$ by ~ 1 % was obtained for this current, whereas in Ref. [58] no effect has been found based on the nuclear wave functions generated by the Argonne v_{18} potential [51]. For the EGM(205) version, the contribution of the short-range weak axial MECs, $\vec{\jmath}_A$(EFT), is strongly enhanced as a consequence of the large value of $\hat{d}^R$.

In Table VI, we compare the results of our IA calculations for the model EM^b with the second row of Table II of Ref. [63]. As it is seen, the agreement between the calculations is very good. On the other hand, the comparison of the final result $\Lambda_{1/2}$ =392.0±2.3 s^{-1} [62] with our Table IV shows reasonable agreement in calculations for the potential model EM^b, whereas the result $\Lambda_{1/2}$ =399±3 s^{-1} [63] indicates the difference of $\sim$ 2 - 3 %. In general, our results exhibit much more model dependence of $\Lambda_{1/2}$, than admitted in Refs. [62, 63].

Let us note that our results for $\Lambda_{1/2}$ contain the factor 1.028(4) taking into account the radiative corrections. These corrections have not yet been calculated within the EFT. The result of "classical" calculations [47] for the inner correction is 0.024(4), valid for the muon capture in any nucleus. The vacuum polarization correction to the muon bound state wave function must be evaluated for every nucleus separately. For the muon capture in deuteron, this correction is $1.80\,\alpha/\pi$=0.0042 [88]. Then the overall radiative corrections for the muon capture in deuteron turn out to be the same as for the muon capture on proton.

TABLE V: Contributions of various components of the currents to $\Lambda_{1/2}$ (in s^{-1}) obtained using chiral potentials EM [65] and EGM [64] for certain values of $\hat{d}^R$. IA($^1S_0$)- the contribution to $\Lambda_{1/2}$ from the $^1S_0$ nn final state and the one-body currents; + $\jmath^0_A$- with the time component of the weak axial MECs added; +$\vec{\jmath}_A$(EFT)- with the space component of the EFT weak axial MECs [44] added; +$\vec{\jmath}_V$- with the space component of the weak vector MECs added; IA(full)- the contribution to $\Lambda_{1/2}$ from all the nn partial waves taken into account and the one-body currents; + $\jmath_A$- with the weak axial MECs [44] added; +$\vec{\jmath}_V$- with the space component of the weak vector MECs added; +$\vec{\jmath}_A$(p.p.c.) - with the weak axial pion potential current added. The values of the doublet capture rate in the last column present in fact $\bar{\Lambda}_{1/2}$.

Potential	$\hat{d}^R$	IA($^1S_0$)	+$\jmath^0_A$	+$\vec{\jmath}_A$(EFT)	+$\vec{\jmath}_V$	IA(full)	+$\jmath_A$	+$\vec{\jmath}_V$	+$\vec{\jmath}_A$(p.p.c.)
EGM(204)	1.57	245.2	244.1	248.3	249.8	384.3	387.3	389.1	387.9
EGM(205)	5.13	241.8	240.7	274.7	276.6	379.5	412.4	414.6	412.7
EM^a	1.18	240.9	240.0	243.0	244.9	379.6	381.6	383.8	381.6
EM^b	2.23	240.9	240.0	248.5	250.5	379.6	387.2	389.4	387.7

TABLE VI: Contributions of the nn partial waves to $\Lambda_{1/2}$ (in s^{-1}), calculated for the model EM^b and with the IA currents. The third row contains the second row of Table II [63].

	$\delta\Lambda_{1/2}(^1S_0)$	$\delta\Lambda_{1/2}(^3P_0)$	$\delta\Lambda_{1/2}(^3P_1)$	$\delta\Lambda_{1/2}(^3P_2)$	$\delta\Lambda_{1/2}(^1D_2)$	$\delta\Lambda_{1/2}(^3F_2)$	$\Lambda_{1/2}$
This work	240.9	22.0	40.9	69.4	6.0	0.4	379.6
Ref. [63]	238.8	21.1	44.0	72.4	4.5	0.9	381.7

IV. CONCLUSIONS

In this work, we studied the doublet capture rate, $\Lambda_{1/2}$, for the reaction $\mu^-(d,\, 2n)\nu_\mu$ (1.10) within the framework of chiral EFT. The nuclear wave functions of the initial and final states were generated from the N^{3}LO chiral potentials of Entem and Machleidt [65] and of Epelbaum, Glöckle and Meißner [64]. The properties of the $^1S_0$ nn state and of the deuteron are presented in Table I and Table II, respectively. The employed weak axial MECs were also constructed within the same EFT scheme [44, 45]. The corresponding LECs, taken consistently with the potentials, are listed in Table III. The short-range part of the weak axial MECs contains one unknown LEC, $\hat{d}^R$ (c_D), which has been constrained earlier [61] by Gazit, Quaglioni and Navrátil in the study of the GT matrix element of the triton β decay and of the static properties of the 3N system, using the same NN potentials and weak axial MECs. With the constant $\hat{d}^R$, constrained in this way and with the same regulator (2.2) entering the weak MECs, we performed rather consistent calculations of $\Lambda_{1/2}$. As it is seen from Table IV, the results are located in two rather distinct intervals, in which the spread of $\Lambda_{1/2}$ is about 2 %. It follows from this result that (i) studying only the triton β decay or the muon capture in deuterium might be insufficient for a precise determination of $\hat{d}^R$, (ii) combined investigation of both reactions can not only provide precise value of $\hat{d}^R$, but will allow for a highly nontrivial test of the chiral EFT framework.

In addition, we studied the influence of the weak axial pion potential current on the $\Lambda_{1/2}$ and $\hat{d}^R$. This current is not a part of the weak axial MECs derived within the HBχPT in Refs. [44, 45], and was not taken into account in the calculations [61] either. As it is seen from our Table IV and Table V, its contribution to $\Lambda_{1/2}$ is non-negligible and can change the value of $\hat{d}^R$ (c_D) up to 7.5 % (44 %). In our opinion, the full consistency of calculations cannot be achieved without including this current also in the study of the reaction (1.8).

What are the possible origins of the observed fairly large spread in the calculated values of $\hat{d}^R$ when using the EGM NN potential of Ref. [64]? First of all, the value of the LEC c_D was obtained in Ref. [61] without taking into account the 3NF in the case of the EGM potentials. Given the significant underbinding of the triton for N^{3}LO NN potentials of Ref. [64] without the inclusion of the 3NF [†], the obtained values for c_D in the case of the EGM NN potentials should be taken with care. Furthermore, while the applied regulator keeps the calculations in the configuration space local, the regulator adopted in the N^{3}LO NN potentials [64, 65]

[†] The underbinding is of the order of $1 \ldots 1.5$ MeV which is larger than in the case of the N^{2}LO potentials.

reads

$$F_\Lambda(p',p) \,=\, e^{-p'^6/\Lambda^6-p^6/\Lambda^6}\,, \quad \Lambda = 0.5\,\mathrm{GeV}\,, \tag{4.1}$$

where p (p') is the initial (final) nucleon momentum in the center-of-mass system. Clearly, this regulator leads to strong non-localities in configuration space. Strictly speaking, only calculations with this type of the regulator can be considered as fully consistent. It is desirable to carry out such calculations in the future in order to see how the form of the regulator affects the results for $\Lambda_{1/2}$ and the values of extracted constant $\hat{d}^R$ (c_D). Another possible source of inconsistency emerges from using two- and three-nucleon forces and the exchange currents at different orders in the chiral expansion. The N^{3}LO NN potentials should be accompanied with the 3NFs calculated at the same order in the chiral expansion. Only recently, the N^{3}LO corrections to the 3NF have become available [89–91]. Moreover, the results of the pioneering work [92] indicate that the inclusion of the long-range N^{3}LO corrections in the 3NF might have strong impact on the values of the LECs c_D and c_E. This issue needs to be investigated in the future. Finally, we applied the weak vector MECs in the leading order only. Evidently, the estimation of higher order terms, derived in Refs. [83–85, 93, 94], is mandatory in future calculations. Last but not least, it would be interesting to carry out the calculations using the N^{2}LO NN potentials and the corresponding 3NF. This would help to obtain a reliable estimation of the theoretical uncertainty for $\Lambda_{1/2}$.

Acknowledgments

We thank P. Navrátil, P. Kammel and L.E. Marcucci for discussions and correspondence. The correspondence with A. Czarnecki is acknowledged. The research by M.T. was partially supported by the Czech Ministry of Education, Youth and Sports within the project LC06002 and by the grant GA ČR P203/11/0701, and the work of R.M. was supported in part by the US Department of Energy under Grant No. DE-FG02-03ER41270. E.E. acknowledges the support by the European Research Council (ERC-2010-StG 259218 NuclearEFT).

[1] E.G. Adelberger *et al.*, Solar fusion cross sections II: the pp chain and CNO cycle, arXiv: 1004.2318.

[2] SNO Collaboration, Q.R. Ahmad *et al.*, Phys. Rev. Lett. **87** (2001) 071301 ; Phys. Rev. Lett. **89** (2002) 011301 ; Phys. Rev. Lett. **89** (2002) 011302 .

[3] SNO Collaboration, S.N. Ahmed *et al.*, Phys. Rev. Lett. **92** (2004) 181301 .

[4] SNO Collaboration, B. Aharmim *et al.*, Phys. Rev. C**72** (2005) 055502 ; Phys. Rev. C**75** (2007) 045502 .

[5] Yu.A. Akulov, B.A. Mamyrin, Phys. Lett. **B610** (2005) 45 .

[6] A.A. Vorobyov *et al.* Hyperfine Interactions **101/102** (1996) 413 .

[7] P. Ackerbauer *et al.* Phys. Lett. **B417** (1998) 224 .

[8] J. Martino, Czech. J. Phys. **B36** (1986) 368 .

[9] M. Cargnelli, PhD thesis, Technical University of Vienna, 1987; W.H. Breunlich, M. Cargnelli, H. Fuhrmann, P. Kammel, J. Marton, J. Werner, J. Zmeskal, C. Petitjean, in Workshop on fundamental μ-physics, Los Alamos, 1986, LA10714C.

[10] MuSun Collaboration, Muon Capture on the Deuteron, http://www.npl.uiuc.edu/exp/musun.
[11] S.L. Adler, R. Dashen, Current Algebras (W.A. Benjamin, New York, 1968).
[12] V. De Alfaro, S. Fubini, G. Furlan, C. Rossetti, Currents in Hadron Physics (North–Holland/American Elsevier, Amsterdam–London/New York, 1973).
[13] J.F. Donoghue, E. Golowich, B.R. Holstein, Dynamics of the Standard Model (Cambridge University Press, Cambridge, 1992).
[14] S. Weinberg, The Quantum Theory of Fields, v. II (Cambridge University Press, Cambridge, 1996).
[15] U.-G. Meissner, Phys. Rep. **161** (1988) 213 .
[16] M. Bando, T. Kugo, K. Yamawaki, Phys. Rep. **164** (1988) 217 .
[17] S. Weinberg, Phys. Rev. **166** (1968) 1568 ; S. Coleman, J. Wess, B. Zumino, Phys. Rev. **177** (1969) 2239 ; C.G. Callan, S. Coleman, J. Wess, B. Zumino, Phys. Rev. **177** (1969) 2247 .
[18] V.I. Ogievetsky, B.M. Zupnik, Nucl. Phys. **B24** (1970) 612 .
[19] E. Ivanov, E. Truhlík, Nucl. Phys. **A316** (1979) 437 .
[20] J. Smejkal, E.Truhlík, H. Göller, Nucl. Phys. **A624** (1997) 655 .
[21] B. Mosconi, P.Ricci, E. Truhlík, Nucl. Phys. **A772** (2006) 81 .
[22] B. Mosconi, P.Ricci, E. Truhlík, P. Vogel, Phys. Rev. C**75** (2007) 044610 .
[23] S. Ciechanowicz, E. Truhlík, Nucl. Phys. **A414** (1984) 508 .
[24] J. Congleton, E. Truhlík, Phys. Rev. C**53** (1996) 956 .
[25] J. Adam Jr. E. Truhlík, S. Ciechanowicz, K.M. Schmitt, Nucl. Phys. **A507** (1990) 675 .
[26] J. Adam Jr. Ch. Hajduk, H. Henning, P.U. Sauer, E. Truhlík, Nucl. Phys. **A531** (1991) 623 .
[27] N. Tatara, Y. Kohyama, K. Kubodera, Phys. Rev. C**42** (1990) 1694 .
[28] P. Ricci, E. Truhlík, B. Mosconi. J. Smejkal, Nucl. Phys. **A837** (2010) 110 .
[29] R. Machleidt, Adv. Nucl. Phys. **19** (1989) 189 .
[30] V.G.J. Stoks, R.A.M. Klomp, C.P.F. Terheggen, J.J. de Swart, Phys. Rev. C**49** (2950) 1994.
[31] S. Nakamura, T. Sato, S. Ando, T.-S. Park, F. Myhrer, V. Gudkov, K. Kubodera, Nucl. Phys. **A707** (2002) 561 .
[32] M. Kirchbach, E. Truhlík, Sov. J. Part. Nucl. **17** (1986) 93 .
[33] I.S. Towner, Phys. Rep. **155** (1987) 263 .
[34] J.-F. Mathiot, Phys. Rep. **173** (1989) 63 .
[35] D.O. Riska, Phys. Rep. **181** (1989) 207 .
[36] T. Ericson, W. Weise, Pions and Nuclei (Clarendon Press, Oxford, 1988).
[37] J. Carlson, R. Schiavilla, Rev. Mod. Phys. **70** (1998) 743 .
[38] D.F. Measday, Phys. Rep. **354** (2001) 243 .
[39] I. Sick, Prog. Part. Nucl. Phys. **47** (2001) 245 .
[40] R. Gilman, F. Gross, J. Phys. **G: Nucl.Part. Phys. 28** (2002) R37 .
[41] S. Weinberg, Physica **96A** (1979) 327.
[42] S. Weinberg, Phys. Lett. **B251** (1990) 292 .
[43] S. Weinberg, Nucl. Phys. **B363** (1991) 3 .
[44] T.-S. Park, K. Kubodera, D.-P. Min, M. Rho, Astrophys. J. **507** (1998) 443 .
[45] D. Gazit, Ph.D. Thesis, The Hebrew University of Jerusalem, 2007, arXiv: 0807.0216; Phys. Lett. **B666** (2008) 472 .
[46] MuCap Collaboration, V.A. Andreev *et al.*, Phys. Rev. Lett. **99** (2007) 032002 .
[47] A. Czarnecki, W.J. Marciano, A. Sirlin, Phys. Rev. Lett. **99** (2007) 032003 .
[48] E. Epelbaum, A. Nogga, W. Glöckle, H. Kamada, U.-G. Meißner, H. Witala, Phys. Rev. C**66**

(2002) 064001 .
[49] B. Mosconi, P. Ricci ,E. Truhlík, Eur. Phys. J.**A25** (2005) 283 .
[50] R. Machleidt, Phys. Rev. C**63** (2001) 024001 .
[51] R.B.Wiringa, V.G.J.Stoks, R.Schiavilla, Phys. Rev. C**51** (1995) 38 .
[52] S.A. Coon, M.D. Scadron, P.C. McNamee, B.R. Barret, D.W.E Blatt, B.H.J. McKellar, Nucl. Phys. **A317** (1979) 242 .
[53] B.S. Pudliner, V.R. Pandharipande, J. Carlson, R.B. Wiringa, Phys. Rev. Lett. **74** (1995) 4396 .
[54] T.-S. Park, L.E. Marcucci, R. Schiavilla, M. Viviani, A. Kievsky, S. Rosati, K. Kubodera, D.-P. Min, M. Rho, Phys. Rev. C**67** (2003) 055206 .
[55] S. Ando, T.-S. Park, K. Kubodera, F. Myhrer, Phys. Lett. **B533** (2002) 25 .
[56] S. Ando, Y.H. Song, T.-S. Park, H.W. Fearing, K. Kubodera, Phys. Lett. **B555** (2003) 49 .
[57] D. Gazit, Phys. Lett. **B666** (2008) 472 .
[58] L.E. Marcucci, M. Piarulli, Few–Body Systems **49** (2011) 35 .
[59] U. van Kolck, Phys. Rev. C**49** (1994) 2932 .
[60] P. Navratil, V. G. Gueorguiev, J. P. Vary, W. E. Ormand, A. Nogga, Phys. Rev. Lett. **99** (2007) 042501 .
[61] D. Gazit, S. Quaglioni, P. Navrátil, Phys. Rev. Lett. **103** (2009) 102502 .
[62] L.E. Marcucci, M. Piarulli, M. Viviani, L. Girlandia, A. Kievsky, S. Rosati, R. Schiavilla, Phys. Rev. C**83** (2011) 014002 .
[63] L.E. Marcucci, A. Kievsky, S. Rosati, R. Schiavilla, M. Viviani, [arXiv:1109.5563 [nucl-th]].
[64] E.Epelbaum, W. Glöckle, U.-G. Meißner, Nucl. Phys. **A747** (2005) 362 .
[65] D.R. Entem, R. Machleidt, Phys. Rev. C**68** (2003) 041001 (R) .
[66] E.Epelbaum, W. Glöckle, U.-G. Meißner, Eur. Phys. J.**A19** (2004) 125 ; Eur. Phys. J.**A19** (2004) 401 .
[67] E.Epelbaum, H.W. Hammer, U.-G. Meißner, Rev. Mod. Phys. **81** (2009) 1773 .
[68] R. Machleidt, D.R. Entem, Phys. Rep. **503** (2011) 1 .
[69] A. Gårdestig, D.R. Phillips, Phys. Rev. C**73** (2006) 014002 .
[70] V. Lensky, V. Baru, E. Epelbaum, C. Hanhart, J. Haidenbauer, A. E. Kudryavtsev, U. -G. Meissner, Eur. Phys. J.**A33** (2007) 339 .
[71] R. Machleidt, I. Slaus, J. Phys. **G: Nucl.Part. Phys. 27** (2001) R69 .
[72] G.A. Miller, M.K. Nefkens, I. Slaus, Phys. Rep. **194** (1990) 1 .
[73] C. van der Leun, C. Alderlisten, Nucl. Phys. **A380** (1982) 261 .
[74] P.J. Mohr, B.N. Taylor, Rev. Mod. Phys. **72** (2000) 351 .
[75] T.E.O. Ericson, M. Rosa-Clot, Nucl. Phys. **A405** (1983) 497 .
[76] J.L. Friar, J. Martorell, D.W.L. Sprung, Phys. Rev. A**56** (1997) 4579 .
[77] N.L. Rodning, L.D. Knudson, Phys. Rev. C**41** (1990) 898 .
[78] M.L. Goldberger, K.M. Watson, Collision Theory, John Wiley and Sons, Inc., New York, 1964.
[79] V. Bernard, Prog. Part. Nucl. Phys. **60** (2008) 82 .
[80] M. C. M. Rentmeester, R. G. E. Timmermans, J. L. Friar, J. J. de Swart, Phys. Rev. Lett. **82** (1999) 4992 .
[81] V. Bernard, N. Kaiser, U.G. Meissner, Int. J. Mod. Phys. **E4** (1995) 193 .
[82] H. Krebs, E. Epelbaum, U. -G. Meissner, Eur. Phys. J.**A32** (2007) 127 .
[83] T.S. Park, D.P. Min, M. Rho, Nucl. Phys. **A596** (1996) 515 .
[84] S. Kölling, E. Epelbaum, H. Krebs, U. -G. Meißner, Phys. Rev. **C80**, 045502 (2009).
[85] S. Kölling, E. Epelbaum, H. Krebs, U.-G. Meißner, [arXiv:1107.0602 [nucl-th]].

[86] N. Fettes, U. -G. Meißner, Nucl. Phys. **A693** (2001) 693 .
[87] P. Navrátil, personal communication, 2011.
[88] A. Czarnecki, personal communication, 2011.
[89] S. Ishikawa, M. R. Robilotta, Phys. Rev. C**76** (2007) 014006 .
[90] V. Bernard, E. Epelbaum, H. Krebs, U. -G. Meissner, Phys. Rev. C**77** (2008) 064004 .
[91] V. Bernard, E. Epelbaum, H. Krebs, U. -G. Meissner, arXiv:1108.3816 [nucl-th].
[92] R. Skibinski, J. Golak, K. Topolnicki, H. Witala, E. Epelbaum, W. Gloeckle, H. Krebs, A. Nogga *et al.*, arXiv:1107.5163 [nucl-th].
[93] S. Pastore, L. Girlanda, R. Schiavilla, M. Viviani, R. B. Wiringa, Phys. Rev. C**80** (2009) 034004 .
[94] S. Pastore, L. Girlanda,R. Schiavilla, M. Viviani, [arXiv:1106.4539 [nucl-th]].
[95] R. Machleidt, in *Computational Nuclear Physics 2: Nuclear Reactions*, eds. K. Langanke, J.A. Maruhn, S.E. Koonin (Springer, New York, 1993), Ch.1, pp. 1-29.

Appendix A: The nn wave functions

Here we discuss in more detail the derivation of the nn wave functions in the formalism of the K-matrix, referring essentially to Ch. 6 and Ch. 7 of Ref. [78] and to Appendix A of Ref. [50].

The basic equation for the nn scattering wave function in terms of the T-matrix is

$$\Psi^+_{\vec{\kappa},S\nu}(\vec{r}) \;=\; \chi_{\vec{\kappa},S\nu}(\vec{r}) + \sum_{S'\nu'} \int \frac{d^3\vec{\kappa}'\chi_{\vec{\kappa}',S'\nu'}}{\epsilon(\kappa)+i\eta-\epsilon(\kappa')} \,\langle \vec{\kappa}', S'\nu'|T|\vec{\kappa}, S\nu\rangle \;, \tag{A1}$$

where the plane wave is defined as

$$\chi_{\vec{\kappa},S\nu}(\vec{r}) \;=\; e^{i\vec{\kappa}\cdot\vec{r}}\, u_{S\nu} \,, \tag{A2}$$

further

$$\epsilon(\kappa) \;=\; \kappa^2/M_n \,, \tag{A3}$$

and $\vec{\kappa}$ (M_n) is the relative nn momentum (neutron mass).

We expand the scattered wave as

$$\Psi^+_{\vec{\kappa},S\nu}(\vec{r}) \;=\; 4\pi \sum_{lJ\nu'l'S'} \left\langle \hat{r}, l'S'\nu'|\mathcal{J}^J|\hat{\kappa}, lS\nu\right\rangle \,\Psi^+_{l'S',\kappa Jl S}(r) u_{S'\nu'} \,, \tag{A4}$$

and the T-matrix as

$$\langle \vec{\kappa}', S'\nu'|T|\vec{\kappa}, S\nu\rangle \;=\; \sum_{ll'J} \left\langle \hat{\kappa}', l'S'\nu'|\mathcal{J}^J|\hat{\kappa}, lS\nu\right\rangle \, T^J_{l'S',lS}(\kappa',\kappa) \,. \tag{A5}$$

Then introducing the definitions

$$\Psi^+_{l',lJ}(r) \;\equiv\; \Psi^+_{l'1,\kappa Jl1}(\kappa, r) \,, \tag{A6}$$

$$T^J_{l',l}(\kappa',\kappa) \;\equiv\; T^J_{l'1,l1}(\kappa',\kappa) \,, \tag{A7}$$

we obtain the equation,

$$\Psi^+_{l',lJ}(r) \;=\; i^{l'} \left\{ \delta_{l',l}\, j_l(\kappa r) + \int \frac{\kappa'^2 d\kappa' j_{l'}(\kappa' r)}{\epsilon(\kappa)+i\eta-\epsilon(\kappa')} \, T^J_{l',l}(\kappa',\kappa) \right\} . \tag{A8}$$

Let us write the function $\Psi^+_{l',lJ}(r)$ as

$$\Psi^+_{l',lJ}(r) \;=\; i^{l'} \, \frac{w^J_{l',l}(\kappa, r)}{\kappa r} \,. \tag{A9}$$

Then from Eq. (A8), one obtains the following equation for the function $w^J_{l',l}(\kappa, r)$

$$\frac{w^J_{l',l}(\kappa, r)}{\kappa r} \;=\; \delta_{l',l}\, j_l(\kappa r) + \int \frac{\kappa'^2 d\kappa' j_{l'}(\kappa' r)}{\epsilon(\kappa)+i\eta-\epsilon(\kappa')} \, T^J_{l',l}(\kappa',\kappa) \,. \tag{A10}$$

It can be shown that the new functions, defined as

$$\bar{w}^J_{l',\alpha}(\kappa,r) \;=\; e^{-i\delta^J_\alpha}\sum_l w^J_{l',l}(\kappa,r)U^J_{l1,\alpha}\,, \tag{A11}$$

satisfy the equations,

$$\frac{\bar{w}^J_{l',\alpha}(\kappa,r)}{\kappa r} \;=\; e^{-i\delta^J_\alpha}\left\{ j_{l'}(\kappa r)U^J_{l'1,\alpha} + \int \frac{\kappa'^2 d\kappa' j_{l'}(\kappa' r)}{\epsilon(\kappa)+i\eta-\epsilon(\kappa')}\sum_l T^J_{l',l}(\kappa',\kappa)U^J_{l1,\alpha}\right\}. \tag{A12}$$

The unitary matrix $U^J_{l1,\alpha}$ is defined as

$$U^J_{l1,\alpha} \;=\; \begin{pmatrix} \cos\,\epsilon^J & -\sin\,\epsilon^J \\ \sin\,\epsilon^J & \cos\,\epsilon^J \end{pmatrix}, \tag{A13}$$

where ϵ^J is the mixing angle. The relation between the T- and K-matrices reads

$$\begin{aligned} T^J_{l',l}(\kappa',\kappa) \;&=\; K^J_{l',l}(\kappa',\kappa) - i\pi M_n\kappa\sum_{l''} K^J_{l',l''}(\kappa',\kappa)T^J_{l'',l}(\kappa,\kappa) \\ &=\; \sum_{l''} K^J_{l',l''}(\kappa',\kappa)[\delta_{l''l} - i\pi M_n\kappa\sum_\alpha U^J_{l''1,\alpha}e^{i\delta^J_\alpha}\cos\delta^J_\alpha K^J_\alpha(\kappa)U^J_{\alpha,l1}]\,. \end{aligned} \tag{A14}$$

Here

$$K^J_\alpha(\kappa) \;\equiv\; K^J_\alpha(\kappa,\kappa) \;=\; -\frac{1}{\pi M_n\kappa}tg\delta^J_\alpha\,. \tag{A15}$$

Using Eq. (A14) in Eq (A12), one obtains for the functions $\bar{w}_{l',J\alpha}(\kappa,r)$ the new set of equations in terms of the K-matrix only

$$\begin{aligned} \frac{\bar{w}^J_{l',\alpha}(\kappa,r)}{\kappa r} \;&=\; \cos\delta^J_\alpha\left\{ j_{l'}(\kappa r)U^J_{l'1,\alpha} + \int \frac{d\kappa'}{\epsilon(\kappa)-\epsilon(\kappa')}\left[\kappa'^2 j_{l'}(\kappa' r)\sum_l K^J_{l',l}(\kappa',\kappa)U^J_{l1,\alpha}\right.\right. \\ &\left.\left. -\kappa^2 j_{l'}(\kappa r)K^J_\alpha(\kappa)U^J_{l'1,\alpha}\right]\right\}. \end{aligned} \tag{A16}$$

It holds that

$$K^J_\alpha(\kappa)U^J_{l'1,\alpha} \;=\; \sum_l K^J_{l',l}(\kappa,\kappa)U^J_{l1,\alpha}\,. \tag{A17}$$

The functions $\bar{w}^J_{l',\alpha}(\kappa,r)$ were computed from Eqs. (A16) by using the program phases [95]. Resolving Eq. (A11) for the functions $w^J_{l',l}(\kappa,r)$, one obtains

$$w^J_{l',l}(\kappa,r) \;=\; \sum_\alpha e^{i\delta^J_\alpha}\,\tilde{U}^J_{\alpha,l1}\,\bar{w}^J_{l',\alpha}(\kappa,r)\,. \tag{A18}$$

Analogously, for the non-coupled channels we have

$$\Psi^+_l(\kappa,r) \;=\; i^l e^{i\delta_l}\frac{w_l(\kappa,r)}{\kappa r}\,, \tag{A19}$$

where the function $w_l(\kappa,r)$ satisfies the equation,

$$\begin{aligned} \frac{w_l(\kappa,r)}{\kappa r} \;&=\; \cos\delta_l\left\{ j_l(\kappa r) + \int \frac{d\kappa'}{\epsilon(\kappa)-\epsilon(\kappa')}\left[\kappa'^2 j_{l'}(\kappa' r)\,K_l(\kappa',\kappa)\right.\right. \\ &\left.\left. -\kappa^2 j_l(\kappa r)K_l(\kappa)\right]\right\}. \end{aligned} \tag{A20}$$

Appendix B: The form factors arising after the Fourier transformation of the weak MECs due to the regulator (2.2)

Here we present the form factors arising due to the regulator (2.2) after the Fourier transformation of the weak MECs containing one boson propagator with the mass m_B.

$$W^n_{0B} \,=\, \frac{2}{\pi x_B}\, I^n_1(x_B,\bar{\Lambda})\,, \tag{B1}$$

$$W^n_{1B} \,=\, \frac{2}{\pi x_B^2}\, \Big[I^n_1(x_B,\bar{\Lambda}) - I^n_2(x_B,\bar{\Lambda}) + x_B\, I^n_3(x_B,\bar{\Lambda})\Big]\,, \tag{B2}$$

$$W^n_{B} \,=\, \frac{2}{\pi x_B^3}\, I^n_4(x_B,\bar{\Lambda})\,, \tag{B3}$$

$$W^n_{2B} \,=\, W^n_{0B} \,+\, \frac{3}{x_B}\, W^n_{1B} \,-\, W^n_B\,, \tag{B4}$$

where

$$I^n_1(x_B,\bar{\Lambda}) \,=\, \int_0^\infty dt\; \frac{t\,\sin(tx_B)}{1+t^2}\; e^{(-t/\bar{\Lambda})^{2n}}\,, \tag{B5}$$

$$I^n_2(x_B,\bar{\Lambda}) \,=\, \int_0^\infty dt\; \cos(tx_B)\; e^{(-t/\bar{\Lambda})^{2n}}\,, \tag{B6}$$

$$I^n_3(x_B,\bar{\Lambda}) \,=\, \int_0^\infty dt\; \frac{\cos(tx_B)}{1+t^2}\; e^{(-t/\bar{\Lambda})^{2n}}\,, \tag{B7}$$

$$I^n_4(x_B,\bar{\Lambda}) \,=\, \int_0^\infty dt\; \sin(tx_B)\, e^{(-t/\bar{\Lambda})^{2n}}\,, \tag{B8}$$

$$x_B \,=\, m_B r\,, \quad \bar{\Lambda} \,=\, \Lambda/m_B\,. \tag{B9}$$

For n=1, Eqs. (A.24)-(A.28) of Section A.2 of Ref. [28] are reproduced.